Elastic Coupling between Nonferroelastic Domain Walls

K. Shapovalov,[1,*] P. V. Yudin,[1] A. K. Tagantsev,[1] E. A. Eliseev,[2] A. N. Morozovska,[3] and N. Setter[1]
[1]Ceramics Laboratory, Swiss Federal Institute of Technology (EPFL), CH-1015 Lausanne, Switzerland
[2]Institute for Problems of Materials Science, National Academy of Sciences of Ukraine, ulitsa Krjijanovskogo, 3, UA-03142 Kiev, Ukraine
[3]Institute of Physics, National Academy of Sciences of Ukraine, prospekt Nauki, 46, UA-03028 Kiev, Ukraine
(Received 20 March 2014; published 12 November 2014)

We reveal a strong elastic interaction between nonferroelastic domain walls in ferroelectric thin films. This interaction, having no analogue in bulk materials, is governed by elastic fields that are associated with the domain walls and extends to distances comparable to the film thickness. Such elastic widening of the nonferroelastic domain walls is shown to be particularly strong in common ferroelectric perovskites. The results are especially relevant for the control of domain wall propagation and the understanding of polarization dynamics.

DOI: 10.1103/PhysRevLett.113.207601 PACS numbers: 77.55.hj, 77.80.bn, 77.80.Dj

Domain walls are an essential attribute of ferroics. Their motion controls to a large extent switching and other properties of ferromagnets and ferroelectrics [1]. The internal structure and properties of the domain walls themselves, accessible at ease only in recent years, are of an increasing interest for both fundamental and applied research [2–7].

The well-known correlation between film thickness and domain wall spacing entails that interactions between adjacent domain walls become substantial upon reduction of the film thickness. Such interaction can be of particular importance for polarization switching where, inevitably, domain walls have to approach closely each other. The interwall interaction was indeed taken into account for ferroelastic (non 180°) domain walls in calculations of domain patterns [8,9] and possibly detected experimentally as well [10]. However, interactions between nonferroelastic (180°) domain walls have been overlooked. Possible interactions between ferroelectric-nonferroelastic domain walls are of high interest since the switching processes in ferroelectric thin films are mainly determined by the motion of nonferroelastic walls because ferroelastic walls typically show poor mobility [11]. Interaction between domain walls is also highly relevant for domain-wall-based agile electronics where it is crucial to precisely control the domain wall's position and movement [12].

In this Letter we address the internal structure of nonferroelastic 180° walls in ferroelectric thin films and its influence on the interaction between these walls. We show that 180° domain walls in ferroelectric films can exhibit an internal structure which is very different from that in the bulk counterparts. We find that the elastic fields associated with the wall extend to a distance comparable with the film thickness, which, in typical situations, is much larger than domain wall thickness in the bulk material. Such elastic fields naturally bring about an appreciable interaction between domain walls. An essential feature of our results is that they have been obtained for a 180° ferroelectric-nonferroelastic wall, while the elastic effects in thin films were commonly expected so far to be important only for ferroelectric-ferroelastic walls.

The predicted effects can be viewed as an impact of the film surface on the domain wall structure. Some surface effects were theoretically addressed in the past, reporting the distortion of the wall structure at distances from the surface comparable with the domain wall thickness [13,14]. In contrast, we find a strong modification of the elastic structure of the wall throughout the whole film thickness, implying an appreciable interwall coupling.

In the following, first we will consider a simple analytical model for the elastic structure of a 180° wall for the case of a freestanding thin film. This simple treatment captures the principle features of the phenomenon both in freestanding thin films and in films on substrates and allows a simple qualitative explanation of the effect to be given. Then we will present the results of a numerical simulation of the wall structures in freestanding films and in films on substrates using an advanced model. Based on these results we evaluate the interwall coupling to show that the force applied to the wall due to this coupling can be comparable to that due to the applied electric field in the switching regime. Our modeling addresses the short-circuited situation for the geometry with top and bottom electrodes, common for applications of ferroelectric thin films. In this situation, the electrostatic effects are strongly suppressed and, as we show, are negligible with respect to the elastic effects in question.

Consider a perovskite ferroelectric film of thickness h in the tetragonal phase, either freestanding or placed on a substrate of thickness $h_S \gg h$ (Fig. 1). Both top and bottom (001) surfaces are electroded and short circuited. This model corresponds to a typical ferroelectric-film-based device where the average depolarizing fields are screened. The film contains one 180° nonferroelastic domain wall oriented along the (100) crystallographic plane and normal to the surface. To describe the elastic effects around the domain wall, we use the thermodynamic Landau theory.

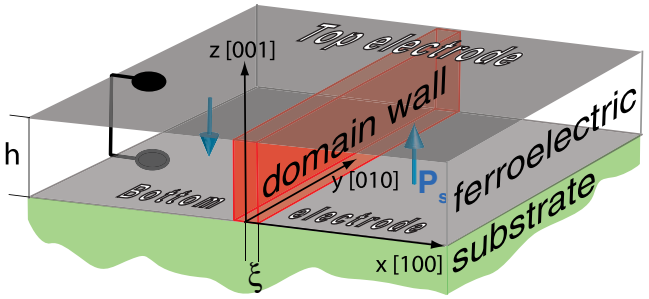

FIG. 1 (color online). Schematic of the problem: thin film of thickness h with a domain wall in the region $x \in (-\xi, \xi)$ on a substrate of thickness h_S in the region $(-h_S < z < 0)$. Two cases considered: $h_S = 0$ (free standing film) and $h_S \gg h$ (film on a substrate).

We introduce the Cartesian reference frame with axes x, z (x_1, x_3) directed as shown in Fig. 1. The Gibbs potential density in a perovskite $(0 < z < h)$ with cubic to tetragonal phase transition ($m\bar{3}m$–$4mm$) can be written in the form [1]

$$G = \frac{1}{2}\alpha P_z^2 + \frac{1}{4}\beta P_z^4 + \frac{1}{6}\gamma P_z^6 - \frac{1}{2}s_{11}(\sigma_{11}^2 + \sigma_{22}^2 + \sigma_{33}^2) - s_{12}(\sigma_{11}\sigma_{22} + \sigma_{22}\sigma_{33} + \sigma_{33}\sigma_{11}) - \frac{1}{4}s_{44}\sigma_{13}^2 - Q_{12}(\sigma_{11} + \sigma_{22})P_z^2 - Q_{11}\sigma_{33}P_z^2 + \frac{1}{2}g_{44}\left(\frac{\partial P_z}{\partial x}\right)^2 + \frac{1}{2}g_{11}\left(\frac{\partial P_z}{\partial z}\right)^2, \quad (1)$$

where P_i is the ferroelectric contribution to the dielectric polarization, σ_{ij} is the stress tensor, α, β, and γ are the 2nd, 4th, and 6th order dielectric stiffnesses, correspondingly, g_{ij} is the correlation energy tensor, s_{ij} is the compliance tensor, and Q_{ij} is the electrostriction tensor. Here, Voigt notation is used for compliance, electrostriction, and correlation energy tensors. For the case of a film on a nonferroelectric substrate, the Gibbs potential in the substrate $(-h_S < z < 0)$ can be written in the same form as in (1) with $P_z = 0$, leaving only elastic terms.

The set of equations to be solved can be obtained from the Gibbs potential using relationships (see, e.g., [1]):

$$\frac{\partial G}{\partial P_i} - \frac{\partial}{\partial x_j}\left(\frac{\partial G}{\partial P_{i,j}}\right) = -\frac{\partial \phi}{\partial x_i}, \quad (2)$$

$$\frac{\partial}{\partial x_i}\left(-\epsilon_b \frac{\partial \phi}{\partial x_i} + P_i\right) = 0, \quad (3)$$

$$-\frac{\partial G}{\partial \sigma_{ij}} = u_{ij}, \quad e_{ikm}e_{jln}\frac{\partial^2 u_{ij}}{\partial x_k \partial x_l} = 0, \quad \frac{\partial \sigma_{ij}}{\partial x_j} = 0, \quad (4)$$

where ϕ is the electrostatic potential defined at $0 < z < h$, $u_{ij} = (U_{i,j} + U_{j,i})/2$ is the strain tensor, U_i is the deformation vector, ϵ_b is the background dielectric permittivity, and e_{ijk} is the Levi-Civita symbol. Hereafter $A_{i,j}$ denotes the derivative of A_i with respect to x_j. The symmetry of the problem allows a 2D treatment with all values dependent on x, z only.

First, we consider the case of a freestanding film with electroded and short-circuited surfaces, with boundary conditions:

$$P_z(x \to \pm\infty) = \pm P_S, \quad (5)$$

$$\phi(z = 0) = 0, \qquad \phi(z = h) = 0, \quad (6)$$

$$\sigma_{ij}(x \to \pm\infty) = 0, \quad (7)$$

$$\sigma_{13}(z = h) = 0, \qquad \sigma_{33}(z = h) = 0, \quad (8)$$

$$\sigma_{13}(z = 0) = 0, \qquad \sigma_{33}(z = 0) = 0, \quad (9)$$

where P_S is the spontaneous polarization value.

To capture the main features and obtain an analytical description for the effect, we present the polarization in the form $P(x, z) = P_b(x) + P_1(x, z)$, where $P_b(x)$ is the solution to the polarization profile in a domain wall in the bulk system and $P_1(x, z)$ is the correction related to the finite film thickness. When calculating the elastic fields near the domain wall that arise due to the electromechanical coupling, we neglect the impact of $P_1(x, z)$ compared to that of $P_b(x)$. As we will see later, such approximation provides a qualitatively correct picture of the phenomenon. Besides, we solve the problem in the approximation of elastically isotropic media ($s_{44} = 2s_{11} - 2s_{12}$) which is also a reasonable approximation [15] for perovskite ferroelectrics (cf. [9]).

The solution for the bulk media may be formally obtained from Eqs. (2)–(5), and (7) as a limiting case $h \to \infty$, for which a 1D treatment is applicable (see, e.g., [14]). For a domain wall in the bulk, the polarization profile $P_b(x)$ can be presented as

$$P_b(x) = P_S f\left(\frac{x}{2\xi}\right), \quad (10)$$

where ξ is the correlation length (2ξ has the meaning of the half-width of the wall), and $f(x)$ is the function describing the polarization profile: $f(x \to \pm\infty) = \pm 1$. For example, for ferroelectrics having second order phase transition not very close to a tricritical point, $f(x) = \tanh(x)$.

To trace the elastic effects around the domain wall, we introduce the relative strain $u_{ij}^r = u_{ij} - u_{ij}^D$, where u_{ij}^D is the strain in the bulk of the domains. For bulk samples and freestanding films, u_{ij}^D is equal to the spontaneous strain $u_{ij}^S = Q_{ij33}P_S^2$. In the case of the bulk material, in view of clamping of all the other strain components by surrounding domains, the only nonzero relative strain component is u_{11}^r:

$$u_{11}^{r,b}(x) = -u_{11}^0 \frac{\Delta P^2(x)}{P_S^2}, \quad (11)$$

$$u_{11}^0 = \frac{s_{11}^2 + s_{11}s_{12} - 2s_{12}^2}{s_{11} + s_{12}} q_{12} P_S^2. \quad (12)$$

Here the notation $\Delta P^2(x) = P_S^2 - P_b^2(x)$ is used, q_{ij} is the elestrostrictive strain coefficient (tensor in Voigt notation) determined as $s_{ijmn}q_{mnkl} = Q_{ijkl}$, and u_{11}^0 is the strain in the middle of the wall. It is seen that for a domain wall in the bulk system, the spacial scales for the polarization profile [Eq. (10)] and for the deformation [Eq. (11)] are the same and determined by the correlation length ξ.

For thin film geometry, according to the aforementioned model, we use the bulk polarization profile $P_b(x)$ in Eq. (1) and thus reduce the problem to the elastic subproblem (4) with boundary conditions (7)–(9). The solution can be found in the framework of the plane-stress approach using stress functions [16,17]. For typical film thicknesses where $h \gg \xi$, one obtains the solution for the relative in-plane strain component in the middle of the film (see Supplemental Material [18]):

$$u_{11}^r(x, h/2) = u_{11}^0\left(-\frac{\Delta P^2(x)}{P_S^2} + \nu R\frac{\xi}{h}g_{11}\left(\frac{x}{h}\right)\right). \quad (13)$$

Here, $\nu = (1/\sqrt{2\pi}\xi)\int_{-\infty}^{\infty}(\Delta P^2(x)/P_S^2)dx = \sqrt{2/\pi}\int_{-\infty}^{\infty}[1 - f^2(x)]dx$ is typically a constant of the order of unity, $R = (q_{11}/q_{12})((s_{11}+s_{12})/(s_{11}+2s_{12})) + (s_{12}/(s_{11}+2s_{12}))$, $g_{11}(\zeta)$ is the dimensionless function controlling the shape of the elastic effects in the middle of the film, which has been obtained analytically in its Fourier form (see Supplemental Material [18]):

$$\widetilde{g_{11}}(\eta) = 2\frac{(\eta/2)\cosh(\eta/2) - (1 + \frac{2s_{12}}{s_{11}})\sinh(\eta/2)}{\eta + \sinh(\eta)}. \quad (14)$$

Expression (13) for the u_{11}^r strain component consists of two terms: the first term, with the scale $x \sim 2\xi$, corresponds to the exact solution for a bulk sample (11); the second term, with the scale h, represents the surface-related contribution to the elastic profile.

Let us compare the two terms in Eq. (13). Since, typically, $h \gg \xi$, the second term is expected to be small by the factor ξ/h. However, in perovskites the factor R is large (e.g., 45 in $PbTiO_3$), which enhances the surface effect. As a result, for typical film thicknesses ($10\xi < h < 100\xi$), the two terms in Eq. (13) are comparable. Such high strength of the surface effect is related to the high anisotropy of the electrostrictive tensor q_{ij}. The high value of R in perovskites is a consequence of the fact that typically $q_{11} \gg q_{12}$ in these materials (e.g., for $PbTiO_3$ $q_{11}/q_{12} = 24.8$).

The elastic profiles for the middle cross section of the film ($z = h/2$), as described by Eq. (13), for free-standing $PbTiO_3$ films with different thicknesses are shown and compared with those of the bulk system in Fig. 2 [19]. One can see an appreciable qualitative difference between the elastic profiles in the film and those in the bulk system. Such a difference holds for a broad range of film thicknesses. Therefore, we can speak here about the effect of "elastic widening" of domain walls in ferroelectric thin films in general.

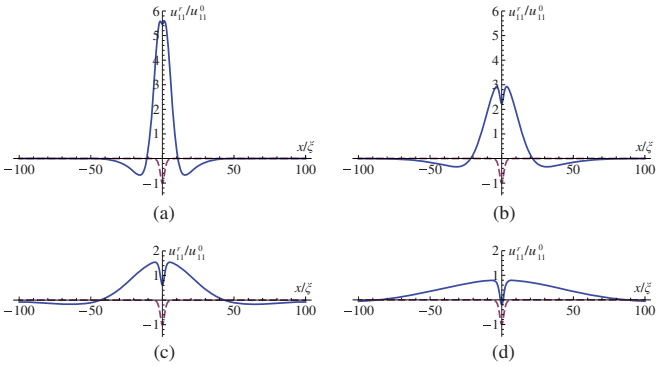

FIG. 2 (color online). Normalized strain component $u_{11}^r(x, h/2)$ calculated according to Eq. (13) as a function of the distance from the wall center x for the middle cross section of a freestanding $PbTiO_3$ film for different film thicknesses h. Dashed lines represent the x dependence of the same component for a wall in the bulk crystal. u_{11}^0 is the strain in the wall center in the bulk system [Eq. (12)]. ξ is the correlation length. (a) $h = 25\xi$, (b) $h = 50\xi$, (c) $h = 100\xi$, and (d) $h = 200\xi$.

The physics behind this effect can readily be elucidated drawing analogy with the Saint-Venant principle [16]. Essentially, the domain wall manifests itself as an inclusion of a material with different lattice constants. The mismatch gives rise to elastic fields which, in agreement with the Saint-Venant principle, penetrate inside the domains on distances of the order of the film thickness. The strain distribution has the well-known structure of elastic fields from a linear indentation [20] on a semi-infinite isotropic medium. These elastic fields are sign changing like those from a vertical point load [17]. In the context of our problem, an effective linear indentation takes place since the bulk solution does not satisfy stress-free conditions on the surfaces [1].

The above considerations capture the main features of the effect. As a support, we performed numerical self-consistent calculations of Eqs. (2)–(9) taking into account the feedback of the elastic fields on the polarization profile and electrostatic effects. The results of the calculations for 20 nm thick films using parameters for $PbTiO_3$ [21] are presented in Fig. 3(a) where the in-plane strain component $u_{11}^r(x)$ is shown. In agreement with the analytical predictions, the elastic fields around the wall extend to distances of the order of the film thickness. In Fig. 3(b) we compare the analytical results with the numerical ones for the middle cross section ($z = h/2$) of the film. One sees that while qualitatively the results obtained with these two methods are in agreement, quantitatively the numerical calculations yield larger values for both the maximal value and the width of the strain profiles, revealing some additional contribution. The source of this contribution is traced back to the feedback of the elastic fields on the polarization profile, which has not been taken into account in the analytical calculations (see Supplemental Material [18]), while the electrostatic contribution to the same effect is shown to be small.

The obtained results for the freestanding film suggest that, in perovskites, the effect related to the finite film

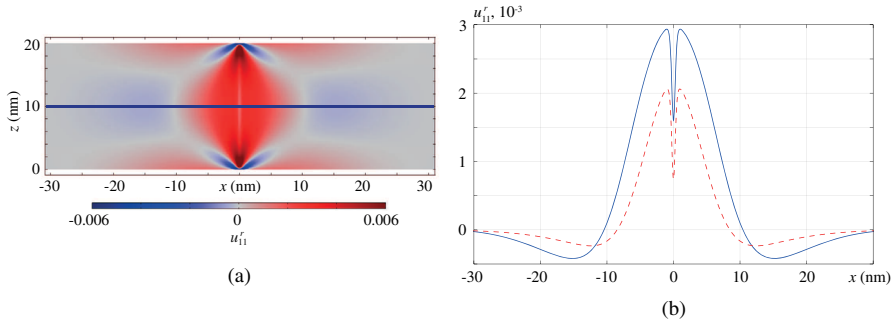

FIG. 3 (color online). In-plane strain $u_{11}^r(x,z)$ for a 20 nm-thick freestanding $PbTiO_3$ film. (a) Strain distribution in the xz cross section. (b) The strain at the middle cross sections of the film: numerical simulations shown by the solid line, Eq. (13) shown as a dashed line.

thickness has high enough value to be observable in the TEM measurements.

Numerical calculations were also run for the case of a thin film on a thick substrate. Equations (2)–(4) with boundary conditions (5)–(8) were solved self-consistently, with additional boundary conditions at the bottom surface of the substrate:

$$u_{11}^r(z=-h_S)=0, U_3(z=-h_S)=0. \tag{15}$$

The elastic properties of the substrate were set identical to those of the film. Calculations were run for different compressive and tensile lattice mismatches between the substrate and the film. Lattice mismatch of magnitudes typical for ferroelectric films was shown to have negligible impact on the relative strain fields near the domain wall [22].

The results of the simulations for a film of thickness 20 nm on a substrate of thickness 100 nm are presented in Fig. 4. One can see that the elastic widening effect manifests itself in the case of a film on a substrate as well, exhibiting strain values comparable to those obtained for the free-standing film, except for the intimate vicinity of the substrate.

The effect of elastic widening of 180° nonferroelastic walls presented above implies an additional mesoscale interaction between them. The force (per unit area) between two domain walls with distance l between them can be obtained from the energy $W(l)$ (per unit length in the third dimension) of their elastic interaction:

$$f(l)=\frac{1}{h}dW/dl, \tag{16}$$

$$W(l)=\iint c_{ijkl}u_{ij}^r(x,z)u_{kl}^r(x-l,z)dxdz, \tag{17}$$

where $u_{ij}^r(x,z)$ is the field created by an individual domain wall located at $x=0$. Equation (17) implies that the elastic field of the ensemble of two domain walls is taken as a sum of those created by individual domain walls. The integration is carried out over all the sample including both film and substrate. Based on our numerical results, we evaluated this force for a $PbTiO_3$ film of thickness 20 nm. Figure 5 shows a plot of the normalized force $E_e(l)=0.5f(l)/P_S$ of interaction between domain walls obtained using Eqs. (16) and (17). The parameter E_e has the meaning of the electric field which creates the same force (per unit area) on the walls as that due to the elastic interaction between domain walls. One should mention that Fig. 5 does not fully describe interaction between domain walls, since it does not take into account the interaction between the polarization profiles of the domain walls. However, one expects that, for $l \gg \xi$, the force acting between the walls due to the elastic widening effect will be dominating. As seen from

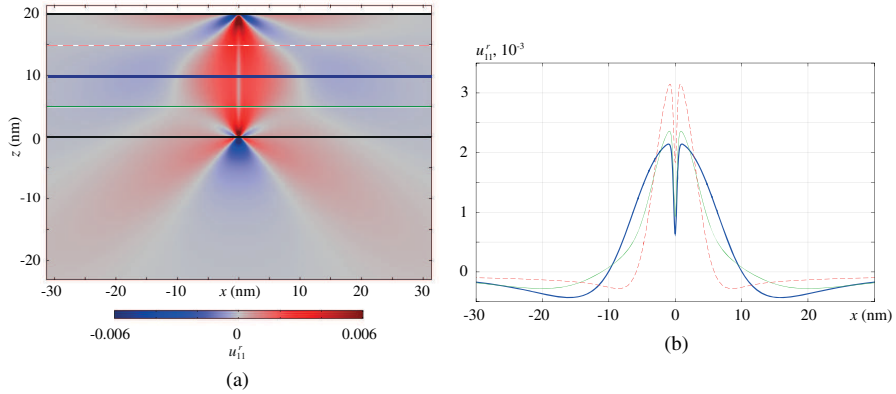

FIG. 4 (color online). In-plane strain $u_{11}^r(x,z)$ in 20 nm-thick $PbTiO_3$ film on a substrate. The thin film lays at $z \in (0,20)$ nm. (a) Strain distribution in xz cross section. (b) Cross sections of $u_{11}^r(x,z)$ at different constant z: in the middle of the film at $z=10$ nm (thick line), at $z=5$ nm (thin line) and $z=15$ nm (dashed line).

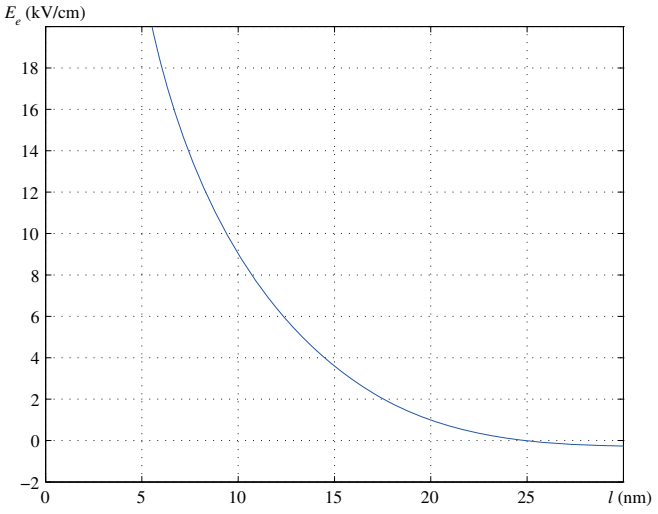

FIG. 5 (color online). The normalized force acting between two 180° domain walls due to the elastic widening effects plotted vs the distance l between them. The units of equivalent out-of-plane electric field E_e which would exert the same pondermotor force on the walls are used (see the text). Calculations are done for a 20 nm $PbTiO_3$ film using Eqs. (16) and (17).

Fig. 5, this force, being equivalent to electric field of a few kV/cm, can be comparable to the coercive force acting on the wall. This suggests a potentially strong effect of the interwall interaction on polarization switching in thin films. Interestingly, the complicated structure of the elastic fields around domain walls allows a weak attraction between the domain walls on distances between them of the order of the film thickness.

It is important to note that the obtained elastic interaction is dominant in thin films with electroded and short-circuited surfaces since the screening of depolarizing fields leads to negligible electrostatic interaction between domain walls (see Supplemental Material [18]).

To conclude, we have demonstrated that in thin ferroelectric films the elastic fields associated with nonferroelastic domain walls extend inside the adjacent domains for a distance comparable to the film thickness. Such elastic widening effect results in appreciable elastic interaction between adjacent walls. We have shown that the predicted interaction between the walls is appreciable for film thicknesses within the range of tens of nanometers.

This interaction could have substantial impact on polarization switching and domain pattern control in ferroelectric thin films. Particularly, the results are relevant for potential agile electronic devices based on domain walls. The fact that domain walls interact with each other opens new possibilities to control their positions and movement.

The research leading to these results has received funding from the European Research Council under the EU 7th Framework Programme (FP7/2007-2013)/ ERC Grant Agreement No. [268058]. This project was supported by the Swiss National Science Foundation Grant No. 200020-144463/1.

*konstantin.shapovalov@epfl.ch

[1] A. Tagantsev, L. Cross, and J. Fousek, *Domains in Ferroic Crystals and Thin Films* (Springer, New York, 2010).
[2] J. Seidel, P. Maksymovych, Y. Batra, A. Katan, S. Y. Yang, Q. He, A. P. Baddorf, S. V. Kalinin, C. H. Yang, J. C. Yang, Y. H. Chu, E. K. H. Salje, H. Wormeester, M. Salmeron, and R. Ramesh, Phys. Rev. Lett. **105**, 197603 (2010).
[3] S. Van Aert, S. Turner, R. Delville, D. Schryvers, G. Van Tendeloo, and E. K. H. Salje, Adv. Mater. **24**, 523 (2012).
[4] L. Goncalves-Ferreira, S. A. T. Redfern, E. Artacho, and E. K. H. Salje, Phys. Rev. Lett. **101**, 097602 (2008).
[5] T. Sluka, A. K. Tagantsev, P. Bednyakov, and N. Setter, Nat. Commun. **4**, 1808 (2013).
[6] J. Seidel *et al.*, Nat. Mater. **8**, 229 (2009).
[7] X.-K. Wei, A. K. Tagantsev, A. Kvasov, K. Roleder, C.-L. Jia, and N. Setter, Nat. Commun. **5**, 3031 (2014).
[8] A. L. Roytburd, J. Appl. Phys. **83**, 239 (1998).
[9] N. A. Pertsev and A. G. Zembilgotov, J. Appl. Phys. **78**, 6170 (1995).
[10] P. Bintachitt, S. Jesse, D. Damjanovic, Y. Han, I. M. Reaney, S. Trolier-McKinstry, and S. V. Kalinin, Proc. Natl. Acad. Sci. U.S.A. **107**, 7219 (2010).
[11] V. Nagarajan, A. Roytburd, A. Stanishevsky, S. Prasertchoung, T. Zhao, L. Chen, J. Melngailis, O. Auciello, and R. Ramesh, Nat. Mater. **2**, 43 (2003).
[12] G. Catalan, J. Seidel, R. Ramesh, and J. F. Scott, Rev. Mod. Phys. **84**, 119 (2012).
[13] S. Conti and E. K. H. Salje, J. Phys. Condens. Matter **13**, L847 (2001).
[14] E. A. Eliseev, A. N. Morozovska, S. V. Kalinin, Y. Li, J. Shen, M. D. Glinchuk, L.-Q. Chen, and V. Gopalan, J. Appl. Phys. **106**, 084102 (2009).
[15] The present analysis is restricted to the isotropic case for simplicity. Numerical simulations confirm that the results for the isotropic case differ only slightly from that for the parameters of $PbTiO_3$ with low elastic anisotropy.
[16] S. Timoshenko and J. Goodier, *Theory of Elasticity* (McGraw-Hill, New York, 1987).
[17] L. Landau, E. Lifshitz, A. Kosevitch, and L. Pitaevski, *Theory of Elasticity* (Butterworth-Heinemann, London, 1986).
[18] See Supplemental Material at http://link.aps.org/supplemental/10.1103/PhysRevLett.113.207601 for details of calculation of widened elastic profiles and for discussion of impact of electrostatics on the interaction between domain walls.
[19] The values used for the ratios $2s_{12}/s_{11} = -0.625$, $q_{11}/q_{12} = 24.8$ correspond to those in $PbTiO_3$. The polarization profile is described by the function $f(x) = \tanh x$.
[20] A. Flamant, C. R. Hebd. Seances Acad. Sci. **114**, 1465 (1892).
[21] Parameters used for $PbTiO_3$: $s_{11} = 8.0 \times 10^{-12}$ Pa^{-1}, $s_{12} = -2.5 \times 10^{-12}$ Pa^{-1}, $s_{44} = 18 \times 10^{-12}$ Pa^{-1}, $Q_{11} = 0.089$ m^4/C^2, $Q_{12} = -0.026$ m^4/C^2, $\alpha = -3.45 \times 10^8$ Vm/C (at $T = 300$ K), $\beta = -2.9 \times 10^8$ Vm^5/C^3, $\gamma = 1.6 \times 10^9$ Vm^9/C^5, $g_{11} = 2 \times 10^{-10}$ Vm^3/C, $g_{44} = 10^{-10}$ Vm^3/C, $\epsilon_b = 100\epsilon_0 = 8.85 \times 10^{-10}$ F/m.
[22] Note that according to our definition of relative strain and due to mechanical coupling of the film on the substrate, $u^r_{11} \to 0$ at $x \to \pm\infty$ for any mismatch.